Astron. Astrophys. 353, 543–556 (2000)

ASTRONOMY AND ASTROPHYSICS

Observations of planetary nebulae in the Galactic Bulge⋆

F. Cuisinier[1], **W.J. Maciel**[2], **J. Köppen**[3], **A. Acker**[4], **and B. Stenholm**[5]

[1] Observatorio do Valongo, Deptartamento de Astronomia, UFRJ, Ladeira do Pedro Antonio 43, 20080 – 090 Rio de Janeiro RJ, Brazil
[2] Instituto Astronômico e Geofisico da USP, Deptartamento de Astronomia, CP 9638, 01065 – 970 São Paulo SP, Brazil
[3] Institut für theoretische Physik und Astrophysik der Universität zu Kiel, 24098 Kiel, Germany
[4] Observatoire de Strasbourg, 11 rue de l' Université, 67000 Strasbourg, France
[5] Lund Observatory, Box 43, 221 00 Lund, Sweden

Received 8 June 1999 / Accepted 30 September 1999

Abstract. High quality spectrophotometric observations of 30 Planetary Nebulae in the Galactic Bulge have been made. Accurate reddenings, plasma parameters, and abundances of He, O, N, S, Ar, Cl are derived.

We find the abundances of O, S, Ar in the Planetary Nebulae in the Galactic Bulge to be comparable with the abundances of the Planetary Nebulae in the Disk, high abundances being maybe slightly more frequent in the Bulge.

The distribution of the N/O ratio does not present in the Galactic Bulge Planetary Nebulae the extension to high values that it presents in the Disk Planetary Nebulae. We interpret this as a signature of the greater age of Bulge Planetary Nebulae.

We thus find the Bulge Planetary Nebulae to be an old population, slightly more metal-rich than the Disk Planetary Nebulae. The population of the Bulge Planetary Nebulae shows hence the same characteristics than the Bulge stellar population.

Key words: ISM: planetary nebulae: general – Galaxy: abundances – Galaxy: center

1. Introduction

Color magnitude diagrams in the Bulge (Ortolani 1998) show without any doubt that the Bulge is an old population – maybe the oldest in the Galaxy.

Chemical abundances in the Bulge can be accessed through tracer populations – Red Giant stars, RR Lyrae and Planetary Nebulae. Since RR Lyrae stars are variable stars occurring only for a certain range of metallicities, their metallicity distribution function is highly biased. On the other hand, red giant stars show a distribution of metallicities as high as that for the solar neighbourhood, or maybe higher (McWilliam & Rich 1994).

Planetary Nebulae (PN) are interesting objects for the study of the Galactic Bulge because they concentrate the energy of their central stars in the emission lines of their spectra, and can therefore be observed relatively easily at this distance. Some of the elements that can be observed in Planetary Nebulae, such as O, S, Ar, reflect the composition of the interstellar medium when the progenitor star was born – and can thus directly be compared with stellar abundances, mainly derived for Fe. Other elements, such as N and He are synthetized in the PN progenitor stars and thus have abundances that are contaminated by the products of this synthesis. These abundances should therefore be indicative of the PN progenitor star *masses*, and therefore *ages*. Ratag et al. (1992, 1997) analysed the spectra of a sample of Galactic Bulge Planetary Nebulae. They found that the oxygen abundance distribution was similar or maybe slightly deficient when compared with the solar neighbourhood one – which is compatible with today's knowledge of the Galactic Bulge star abundances. They found as well that the N/O ratio was higher for Galactic Bulge Planetary Nebulae than for the Disk ones, which requires (1) that the Galactic Bulge Planetary Nebulae progenitors were younger than the Disk ones, in contradiction with the stellar data, or (2) that the PN progenitor star nucleosynthesis history was different in the Bulge and in the Disk.

The Ratag et al. (1992, 1997) sample is however of very uneven quality: in many spectra, important diagnostic lines as [OIII] 436.2 nm or [NII] 575.5 nm are missing. This motivated us to obtain a sample of high quality PN spectra.

2. Observations and reductions

Belonging to the Galactic Bulge can be a tricky question, because of the contamination of foreground objects. For Planetary Nebulae, clear criteria have been identified by Acker et al. (1991), that, according to them, allow to reduce the contamination of foreground objects down to less than 10%. These criteria are: (i) diameter smaller than 10 arcsec, (ii) coordinates within 5 degrees of the galactic center, and (iii) flux at 6cm less than 100 mJy. We have built a sample of Planetary Nebulae in the direction of the Bulge responding as far as possible to the criteria identified by Acker et al. (1991).

We obtained spectra for a sample of 30 Planetary Nebulae responding to these criteria. The only PN of our sample that does not respond to these criteria is PN G 351.1 + 04.8 (M 1 - 19), but although it is not within 5 degrees of the galactic center, it is quite close, and it agrees with all the other criteria. Thus, we

Send offprint requests to: F. Cuisinier (cuisinie@sun1.ov.ufrj.br)

⋆ based on observations made at ESO, La Silla, Chile

can assume that most of the PN of our sample actually belong to the Galactic Bulge.

The observations were made at the European Southern Observatary 1.52m telescope in La Silla, Chile, in two observing runs, in July 1995 and in July 1996. The instrument used was the B&C spectrograph with the grating #23, and the CCD 2K chip FA#24, giving a spectral coverage of the range 380–750 nm, with a resolution of 0.6 nm. Such a resolution allowed us to separate clearly the [SII] 671.6, 673.1 nm lines, and [OIII] 436.3 nm, Hβ. The sky apperture we used was of 3×4arcsec.

Because of the high interstellar reddening towards the Galactic Bulge, high quality spectra are difficult to obtain: weak lines that are indispensable for the plasma diagnosis, like [OIII] 436.3 nm or [NII] 575.5 nm are so reddenned that they cannot be observed in good conditions (let us say, at S/N$\geq$ 10) without saturating the most intense ones, as Hα or [OIII] 500.7 nm.

Thus, for each PN, we obtained (i) one spectrum with the weak lines, at least [NII] 575.5 nm, observed in good conditions, which required exposures times varying between 45 and 90 mn, (ii) one spectrum with the strongest lines unsaturated, typically with exposure times of 5 minutes.

Each night 3–4 observations of one or several of the following spectrophotometric standard flux stars were made: LTT 377, LTT 7379, Feige 110, CD -32 9927, and Kopff 27. References of their fluxes distributions were taken from Baldwin & Stone (1984), Stone & Baldwin (1983), Colina & Bohlin (1994), Hamuy et al. (1992, 1994), Massey et al. (1988), Oke (1990), Stone (1977, 1996).

The spectra have been reduced in wavelength and in flux with the MIDAS package. The lines have been measured with the IRAF package. Some of the lines we observed, although separated, suffered partial blending: [SII] 671.6, 673.1 nm and [OII] 732,733 nm (as a matter of fact [OII] 732,733 nm is a quadruplet: 731.8, 731.9, 733.0, 733.1 nm. But at our resolution, we were only able to separate the two doublets). These lines were properly deconvolved for partial blending with multiple gaussian fitting. [OIII] 436.3 nm and Hβ were clearly separated, so they did not require any deblending.

The line intensities are presented in Table 1.

3. Plasma diagnosis and abundance determinations

3.1. Presentation of our data

The interstellar reddenings and the plasma parameters (electronic temperatures, electronic densities) were derived with the plasma diagnosis code HOPPLA (Köppen et al. 1991). The interstellar reddenings were derived using the Balmer line ratios. For all PN of our sample, Hα and Hβ could be measured in good conditions, and in most cases, Hγ and Hδ as well. The dereddened Balmer lines fitted always within 15% of the case B predicted values.

Electronic temperatures have been derived for the [NII] zone and, when possible, for the [OIII] zone. When the [OIII] 436.3 nm was too weak to be measurable in good conditions, the [OIII] zone electronic temperature was assumed to be the same as in the [NII] zone.

The electronic densities were derived using the [SII] 671.6, 673.1 nm line ratio.

The adopted plasma parameters, interstellar reddenings and excitation classes of the PN of this sample are presented in Table 2.

Elemental abundances were derived from the ionic abundances using ionisation correction factors (ICF). The ICF we used are described in Köppen et al. 1991. The abundances we derived for the PN of our sample are presented in Table 3.

3.2. Internal uncertainties

Uncertainties on the measured spectra originate from various sources, random and systematic. The random uncertainties can be divided between: (i) the uncertainty on the determination of the atmospheric transmission, (ii) the CCD read–out noise, and (iii) the photon shooting noise. Cuisinier et al. (1992) showed that the total derived response of the instrument, with the atmospheric transmission, was constant within 5% over 100nm. The exposure times were chosen appropriately, so that the CCD read-out noise can be neglected. Thus, the main random error source should be the photon shooting noise, which dominates the line measurement uncertainties, through the uncertainty on the continuum level setting.

In order to evaluate random uncertainties on the plasma parameters and abundances we derived, we performed Monte-Carlo simulations, adding gaussian noise to the observed spectra. Random values have been added and subtracted to each of the lines of each of the observed observed spectra. For each spectrum, 200 shots have been made. A visual inspection of our spectra showed that the noise level was fairly constant over the wavelength range, showing only a notable increase at the ends of the range, due to the loss of efficiency of the spectrograph at high grating angles.

The level of the gaussian noise we added to the spectra was based on our visual evaluation of the uncertainty on the line measurements. We adopted standard deviations for the random values we added to the spectra reproducing our evaluation of the noise level. We divided the spectra in three classes: A, B, and C. C having an uncertainty level of 2% in Hβ units, B 1%, and A less than 0.5%.

Table 2 presents the standard deviations on each of the plasma parameters for each spectrum that we derived. For the density, in cases where the evaluated density reaches the saturation limits of the sulfur lines (taken as $100\mathrm{cm}^{-3}$ for the low density limit and $20{,}000\mathrm{cm}^{-3}$ for the high density limit), these values of the standard deviations should just be seen as indications. No values have been generated over the high-density limit (or below the low density one), resulting sometimes for the concerned spectra in highly non–gaussian distributions of the random generated densities.

Table 3 presents the standard deviations on each of the abundances for each spectrum that we derived.

Fig. 1 shows the resulting 1σ uncertainties on the abundances as a function of the abundances themselves, for various excitation classes.

Table 1. Line intensities of the observed planetary nebulae, relatively to $H\beta = 100$. Quality classes are presented as well (see text).

$\lambda\lambda$ (Å)	PNG qual.:	$000.1+04.3$ C	$000.2-01.9$ A	$000.7+03.2$ C	$001.2-03.0$ A	$001.4+05.3$ B	$002.6-03.4$ A	$002.7-04.8$ A	$005.0+04.4$ A
4026	He I	-	-	-	-	-	-	-	1.3
4072	[S II]	-	-	-	-	-	-	-	2.1
4102	H I	-	10.8	-	12.6	13.6	13.6	17.7	11.1
4190	O II	-	-	-	-	-	-	-	-
4267	C II	-	-	-	-	-	-	-	0.5
4340	H I	18.2	27.1	-	27.7	28.7	29.2	33.9	24.8
4363	[O III]	6.6	-	-	-	-	-	-	1.0
4388	He I	-	-	-	-	-	-	-	0.5
4472	He I	-	3.8	-	-	-	-	5.8	4.9
4639	O II	-	-	-	-	-	-	-	-
4686	He II	10.5	-	29.6	-	-	-	9.9	-
4711	[Ar IV]+blend	-	-	-	-	-	-	-	1.8
4740	[Ar IV]	4.4	-	3.6	-	-	-	1.0	0.6
4861	H I	100	100	100	100	100	100	100	100
4922	He I	-	-	-	-	-	-	2.0	-
4959	[O III]	678	79.5	281	-	130	-	170	254
5007	[O III]	2171	242	882	-	315	-	519	808
5199	[N I]	-	0.6	-	1.5	-	1.6	3.7	0.7
5271	[FeII],[FeIII]	-	-	-	-	-	-	-	-
5399	0 IV	-	-	-	-	-	0.2	-	-
5412	He II	3.3	-	5.5	-	-	-	1.3	-
5518	[Cl III]	-	0.8	-	-	-	-	0.8	0.3
5538	[Cl III]	-	0.8	-	-	-	-	0.8	1.5
5603	?	-	-	-	-	-	-	-	-
5614	?	-	-	-	-	-	-	-	-
5667	N II	-	-	-	-	-	-	0.7	-
5676	N II	-	-	-	-	-	-	-	-
5696	C III	-	-	-	2.4	-	3.2	-	-
5754	[N II]	5.0	2.8	5.5	1.3	0.8	1.3	4.1	5.7
5773	C III	0.6	-	-	-	-	-	-	-
5801	C IV	-	-	-	-	-	-	-	-
5812	C IV	-	-	-	-	-	-	-	-
5876	He I	52.8	37.9	47.4	3.1	33.8	3.2	33.7	60.7
5932	He II	-	-	-	-	-	-	0.3	-
6046	O I?	-	-	-	-	-	0.3	-	-
6102	[K IV]	-	-	-	-	-	-	-	-
6300	[O I]	40.9	6.8	20.1	3.4	-	2.7	6.7	10.6
6312	[S III]	10.8	2.8	7.3	-	1.8	-	2.0	5.6
6347	Si II	-	-	-	-	-	-	-	0.4
6364	[O I]	15.7	2.4	7.7	1.1	-	1.0	2.6	3.9
6437	[Ar V]	2.2	-	-	-	-	-	-	-
6462	?	-	-	-	-	-	-	0.5	-
6548	[N II]	76.0	147	308	230	36.4	191	150	159
6563	H I	1836	1038	1407	954	848	700	553	1179
6583	[N II]	240	464	1008	716	115	600	461	512
6678	He I	27.9	16.4	26.3	-	13.2	-	12.4	25.9
6716	[S II]	18.5	39.1	62.0	27.2	5.9	16.1	30.0	8.0
6731	[S II]	35.9	56.1	94.5	53.4	7.3	32.2	37.1	17.3
7006	[Ar V]	8.0	-	4.0	0.5	-	0.4	-	-
7065	He I	78.7	17.4	26.3	1.6	15.8	1.4	8.3	51.0
7136	[Ar III]	178	54.6	189	1.3	46.3	0.7	40.8	132
7178	He II	-	-	-	-	-	-	-	-
7281	He I	-	-	-	-	-	-	-	4.3
7320	[O II]	120	17.4	20.1	2.5	13.8	1.9	5.4	20.1
7330	[O II]	95.4	14.4	16.1	1.8	11.3	1.4	4.9	17.0

Table 1. (continued)

$\lambda\lambda$ (Å)	PNG qual.:	$351.1+04.8$ A	$355.1-02.9$ A	$355.2-02.5$ A	$355.4-02.4$ B	$355.6-02.7$ A	$355.7-03.0$ A	$356.2-04.4$ A	$356.5-03.9$ A
4026	He I	-	-	-	-	-	1.2	-	-
4072	[S II]	1.5	-	1.7	-	-	2.9	2.4	-
4102	H I	16.8	11.0	12.4	12.2	11.1	12.7	18.6	12.3
4190	O II	-	-	-	-	0.8	-	-	-
4267	C II	0.3	-	-	-	-	0.9	-	-
4340	H I	34.4	24.9	28.3	26.1	25.8	27.9	35.5	29.2
4363	[O III]	1.0	9.3	3.6	2.0	3.9	1.9	7.8	-
4388	He I	0.5	-	0.4	-	-	0.6	0.6	-
4472	He I	4.7	3.6	3.7	4.4	3.6	4.3	4.5	1.4
4639	O II	-	-	-	-	-	-	-	-
4686	He II	1.4	3.9	-	13.3	-	2.2	4.3	-
4711	[Ar IV]+blend	1.4	-	1.5	-	1.4	-	-	-
4740	[Ar IV]	-	4.6	-	2.5	-	1.8	2.9	-
1 4861	H I	100	100	100	100	100	100	100	100
4922	He I	-	-	-	-	-	1.6	1.3	-
4959	[O III]	169	653	371	305	330	309	556	7.0
5007	[O III]	520	2031	1237	947	1021	982	1693	22.8
5199	[N I]	0.2	-	1.0	3.3	-	0.9	0.3	-
5271	[FeII],[FeIII]	0.2	-	-	0.4	0.2	-	0.1	-
5399	0 IV	-	-	-	-	-	-	-	-
5412	He II	0.1	0.6	-	2.2	-	-	0.5	-
5518	[Cl III]	0.5	0.4	0.7	1.1	0.5	0.8	0.5	0.3
5538	[Cl III]	0.9	1.1	1.3	2.0	1.0	1.2	0.9	0.5
5603	?	-	-	-	0.4	-	-	-	-
5614	?	-	-	-	-	-	-	-	-
5667	N II	-	-	-	0.3	-	-	-	-
5676	N II	-	-	-	-	-	0.5	-	-
5696	C III	-	-	-	-	-	-	-	0.7
5754	[N II]	1.5	4.2	4.1	6.8	2.3	3.2	1.3	3.0
5773	C III	-	-	-	-	-	-	-	-
5801	C IV	0.8	-	-	-	-	-	-	-
5812	C IV	0.6	-	-	-	-	-	-	-
5876	He I	30.0	41.2	41.5	49.5	37.3	44.5	28.2	13.0
5932	He II	-	-	-	-	-	-	-	-
6046	O I?	-	-	-	-	-	-	-	-
6102	[K IV]	-	-	-	-	-	-	0.2	-
6300	[O I]	2.1	24.0	19.3	21.7	10.8	13.8	6.1	4.2
6312	[S III]	2.4	7.3	4.8	6.0	4.8	4.2	3.5	1.4
6347	Si II	0.2	-	-	-	-	-	-	-
6364	[O I]	0.7	8.6	6.4	8.5	3.7	4.7	2.2	1.3
6437	[Ar V]	-	-	-	-	-	-	-	-
6462	?	-	-	-	-	-	-	-	-
6548	[N II]	58.1	51.7	91.8	328	29.2	91.5	20.5	133
6563	H I	665	1063	981	1055	960	954	594	768
6583	[N II]	182	163	294	1010	90.7	291	63.0	419
6678	He I	10.7	16.8	16.4	22.2	14.9	17.5	9.2	5.0
6716	[S II]	5.5	7.5	11.6	43.9	4.7	22.1	3.6	16.3
6731	[S II]	10.6	15.6	20.5	73.0	9.0	36.8	7.0	31.8
7006	[Ar V]	-	-	-	0.6	-	-	-	-
7065	He I	13.2	-	28.5	31.9	41.7	19.2	16.5	7.6
7136	[Ar III]	36.4	-	57.1	146	58.6	64.4	32.7	12.0
7178	He II	-	-	-	-	-	-	-	-
7281	He I	1.6	-	3.4	-	-	2.4	-	-
7320	[O II]	6.8	48.1	27.9	18.9	46.1	10.8	7.5	29.6
7330	[O II]	5.8	38.8	23.5	16.1	39.8	9.4	6.3	26.0

Table 1. (continued)

$\lambda\lambda$ (Å)	PNG qual.:	$356.5-02.3$ A	$357.4-03.5$ A	$357.4-03.2$ B	$358.2+03.5$ A	$358.2+03.6$ A	$358.2+04.2$ C	$358.3+03.0$ B	$358.7-05.2$ A
4026	He I	-	-	1.7	-	-	-	-	-
4072	[S II]	-	-	3.6	1.2	-	-	-	-
4102	H I	-	-	14.0	10.5	12.0	11.7	-	16.5
4190	O II	-	-	-	-	-	-	-	-
4267	C II	-	-	-	-	-	-	-	-
4340	H I	26.0	-	28.0	24.5	27.2	26.2	-	31.1
4363	[O III]	-	-	2.8	5.6	7.8	-	-	9.7
4388	He I	-	-	-	-	3.4	-	-	-
4472	He I	-	3.8	4.1	3.0	-	4.9	-	3.6
4639	O II	-	-	-	-	-	-	-	-
4686	He II	-	-	15.3	1.2	11.3	-	3.2	9.8
4711	[Ar IV]+blend	-	-	5.5	-	-	-	-	-
4740	[Ar IV]	-	-	2.7	2.3	4.8	-	5.1	5.0
4861	H I	100	100	100	100	100	100	100	100
4922	He I	-	1.3	1.7	-	1.4	-	-	1.2
4959	[O III]	-	164	375	467	567	217	633	589
5007	[O III]	-	540	1171	1442	1763	689	1980	1812
5199	[N I]	-	-	1.9	-	-	-	-	0.6
5271	[FeII],[FeIII]	-	-	-	-	-	-	-	-
5399	0 IV	-	-	-	-	-	-	-	-
5412	He II	-	-	2.2	-	2.0	-	-	1.4
5518	[Cl III]	-	0.6	1.1	0.5	0.8	-	-	0.6
5538	[Cl III]	-	1.1	1.8	0.8	1.3	-	-	1.4
5603	?	-	-	-	-	-	-	-	-
5614	?	-	-	-	1.9	-	-	-	-
5667	N II	-	-	-	-	-	-	-	-
5676	N II	-	-	-	-	-	-	-	-
5696	C III	2.0	-	-	-	-	-	-	-
5754	[N II]	2.4	2.0	6.6	1.2	3.5	3.9	12.4	2.9
5773	C III	-	-	-	-	-	-	-	-
5801	C IV	-	-	-	-	-	-	-	-
5812	C IV	-	-	-	-	-	-	-	-
5876	He I	3.4	34.5	41.3	45.6	36.9	52.1	63.2	26.5
5932	He II	-	-	-	-	-	-	-	-
6046	O I?	-	-	-	-	-	-	-	-
6102	[K IV]	-	-	-	-	0.7	-	-	0.4
6300	[O I]	4.4	3.6	19.1	8.7	18.6	7.8	44.4	13.1
6312	[S III]	-	3.0	6.9	5.1	6.1	3.6	17.8	4.2
6347	Si II	-	-	-	-	-	-	-	-
6364	[O I]	1.7	1.2	6.8	2.9	6.4	-	16.2	4.6
6437	[Ar V]	-	-	-	-	0.7	-	-	-
6462	?	-	-	-	-	-	-	-	-
6548	[N II]	258	53.2	238	24.5	56.5	128	140	38.2
6563	H I	1221	828	966	1440	1033	1204	1786	611
6583	[N II]	817	168	875	76.3	172	407	440	118
6678	He I	-	12.8	16.4	22.2	15.4	23.6	29.5	9.0
6716	[S II]	42.5	6.1	29.3	5.8	11.2	13.7	13.7	6.9
6731	[S II]	82.2	11.4	52.8	11.5	22.0	26.2	29.5	13.2
7006	[Ar V]	0.8	-	-	-	2.4	-	1.3	1.1
7065	He I	0.7	26.7	22.6	37.8	31.8	27.7	92.7	18.5
7136	[Ar III]	3.0	45.3	102	14.9	76.7	108	221	40.9
7178	He II	-	-	0.7	-	-	-	-	-
7281	He I	-	-	2.6	4.6	-	-	-	-
7320	[O II]	13.6	40.3	13.6	20.8	36.2	25.1	100	28.9
7330	[O II]	11.8	32.0	10.7	16.2	30.3	19.7	83.4	22.0

Table 1. (continued)

$\lambda\lambda$ (Å)	PNG qual.:	$358.9+03.2$ B	$358.9+03.4$ B	$359.1-02.3$ B	$359.3-03.1$ B	$359.7-02.6$ B	$359.7-01.8$ C
4026	He I	-	-	-	-	-	-
4072	[S II]	-	-	-	-	-	-
4102	H I	-	-	12.6	12.0	-	-
4190	O II	-	-	-	-	-	-
4267	C II	-	-	-	-	-	-
4340	H I	-	-	29.7	27.8	-	20.8
4363	[O III]	-	-	0.9	-	-	11.2
4388	He I	-	-	-	-	-	-
4472	He I	3.6	-	4.1	2.8	-	-
4639	O II	0.3	-	-	-	-	-
4686	He II	1.8	-	-	-	-	22.5
4711	[Ar IV]+blend	-	-	-	-	-	-
4740	[Ar IV]	-	-	-	-	-	-
4861	H I	100	100	100	100	100	100
4922	He I	-	-	-	1.4	-	-
4959	[O III]	365	148	230	26.1	353	500
5007	[O III]	1164	480	713	85.2	1131	1584
5199	[N I]	1.2	-	-	-	4.3	-
5271	[FeII],[FeIII]	-	-	-	-	-	-
5399	0 IV	-	-	-	-	-	-
5412	He II	-	-	-	-	-	-
5518	[Cl III]	0.9	-	-	0.3	-	-
5538	[Cl III]	2.1	-	-	0.7	-	-
5603	?	-	-	-	-	-	-
5614	?	-	-	-	-	-	-
5667	N II	-	-	-	-	-	-
5676	N II	-	-	-	0.5	-	-
5696	C III	-	-	-	1.0	-	-
5754	[N II]	7.2	14.0	1.6	2.6	5.7	-
5773	C III	-	-	-	-	-	-
5801	C IV	-	-	-	-	-	-
5812	C IV	-	-	-	-	-	-
5876	He I	64.2	69.5	35.9	34.4	66.2	34.8
5932	He II	-	-	-	-	-	-
6046	O I?	-	-	-	-	-	-
6102	[K IV]	-	-	-	-	-	-
6300	[O I]	20.0	11.6	8.2	1.7	15.1	7.3
6312	[S III]	8.4	6.7	3.0	2.6	10.5	7.3
6347	Si II	0.9	-	-	-	-	-
6364	[O I]	7.5	3.7	2.3	-	6.2	-
6437	[Ar V]	-	-	-	-	-	-
6462	?	-	-	-	-	-	-
6548	[N II]	294	433	65.0	176	96.8	27.0
6563	H I	1597	1680	1065	1143	1840	1704
6583	[N II]	941	1321	204	567	305	82.0
6678	He I	31.0	32.9	15.8	14.5	31.5	18.5
6716	[S II]	41.2	17.7	21.3	16.9	7.8	17.4
6731	[S II]	73.7	37.8	27.0	28.7	17.1	21.3
7006	[Ar V]	-	-	-	-	-	3.4
7065	He I	60.6	77.4	16.2	14.0	86.5	25.3
7136	[Ar III]	227	232	45.3	36.1	148	71.5
7178	He II	-	-	-	-	-	4.5
7281	He I	-	-	-	2.5	-	-
7320	[O II]	34.3	71.3	19.0	17.6	68.0	18.0
7330	[O II]	28.1	56.1	15.8	14.1	55.0	14.6

Table 2. Reddenings (c) and plasma parameters (temperatures, densities) of the observed spectra. These data are given after the PN G names, the commen names, and our evaluation of the quality of the spectra. Excitation classes (EC) are as well given. All the parameters are followed by our evaluations of the uncertainties by Monte–Carlo simulations (1σ). The temperatures are given in units of 10^4K, for the [OIII] and [NII] zones. The densities, derived from the [SII] lines ratio, are given in $10^3\,\mathrm{cm}^{-3}$.

PN G	usual name	qual.	c	σ_c	T(OIII)	$\sigma_{T(OIII)}$	T(NII)	$\sigma_{T(NII)}$	n(SII)	$\sigma_{n(SII)}$	EC
$000.1+04.3$	H 1-16	C	2.50	±0.02	1.00	±0.09	1.41	±0.30	7.30	±6.0	6
$000.2-01.9$	M 2-19	A	1.77	±0.01	-	-	0.80	±0.05	1.86	±0.1	3
$000.7+03.2$	He 2-250	C	2.11	±0.03	-	-	0.80	±0.09	2.29	±0.4	7
$001.2-03.0$	H 1-47	A	1.56	±0.01	-	-	0.56	±0.04	7.04	±1.1	<2
$001.4+05.3$	H 1-15	B	1.45	±0.04	-	-	0.83	±0.27	1.16	±1.8	4
$002.6-03.4$	M 1-37	A	1.15	±0.01	-	-	0.56	±0.04	8.13	±2.7	<2
$002.7-04.8$	M 1-42	A	0.88	±0.01	-	-	0.86	±0.04	1.17	±0.1	6
$005.0+04.4$	H 1-27	A	1.89	±0.01	0.74	±0.09	0.89	±0.04	19.27	±4.7	5
$351.1+04.8$	M 1-19	A	1.11	±0.01	0.78	±0.09	0.82	±0.09	6.76	±5.8	4
$355.1-02.9$	H 1-31	A	1.78	±0.01	1.05	±0.02	1.38	±0.11	12.47	±5.2	6
$355.2-02.5$	H 1-29	A	1.65	±0.01	0.92	±0.04	1.07	±0.05	4.41	±1.2	5
$355.4-02.4$	M 3-14	B	1.74	±0.01	0.85	±0.10	0.82	±0.04	3.30	±0.4	6
$355.6-02.7$	H 1-32	A	1.64	±0.01	0.99	±0.04	1.41	±0.19	7.45	±6.0	5
$355.7-03.0$	H 1-33	A	1.61	±0.01	0.82	±0.04	0.98	±0.06	3.38	±0.4	5
$356.2-04.4$	Cn 2-1	A	0.98	±0.01	0.98	±0.04	1.17	±0.31	6.85	±8.1	6
$356.5-03.9$	H 1-39	A	1.31	±0.01	-	-	0.79	±0.04	7.50	±2.3	2
$356.5-02.3$	M 1-27	A	1.90	±0.03	-	-	0.64	±0.11	6.53	±3.2	<2
$357.4-03.5$	M 2-18	B	1.41	±0.01	-	-	0.95	±0.09	7.47	±4.2	6
$357.4-03.2$	M 2-16	B	1.62	±0.01	0.87	±0.08	0.85	±0.04	4.81	±1.1	6
$358.2+03.5$	H 2-10	A	2.18	±0.01	1.04	±0.05	1.16	±0.24	8.39	±6.0	5
$358.2+03.6$	M 3-10	A	1.73	±0.01	1.04	±0.02	1.24	±0.10	8.20	±3.6	6
$358.2+04.2$	M 3-8	C	1.92	±0.03	-	-	0.92	±0.18	6.51	±6.7	4
$358.3+03.0$	H 1-17	B	2.48	±0.01	-	-	1.52	±0.11	18.18	±4.7	6
$358.7-05.2$	H 1-50	A	1.04	±0.01	1.04	±0.02	1.28	±0.13	7.40	±5.0	6
$358.9+03.2$	H 1-20	B	2.29	±0.01	-	-	0.89	±0.04	4.59	±0.7	5
$358.9+03.4$	H 1-19	B	2.36	±0.01	-	-	0.93	±0.04	15.85	±4.9	4
$359.1-02.3$	M 3-16	B	1.73	±0.02	0.75	±0.16	0.89	±0.16	1.22	±0.3	4
$359.3-03.1$	M 3-17	B	1.83	±0.02	-	-	0.74	±0.08	3.46	±1.2	3
$359.7-02.6$	H 1-40	B	2.50	±0.02	-	-	1.18	±0.13	20.00 H	-	5
$359.7-01.8$	M 3-45	C	2.42	±0.03	1.35	±0.93	-	-	1.25	±0.9	6

3.2.1. Uncertainties on the oxygen abundances

Taking away the 3 PN with very high uncertainties, a systematic tendency to an increase of the uncertainty on the oxygen abundance for high oxygen abundances can be seen: if the uncertainty is clearly lower than 0.2 dex for low oxygen abundances (O $\simeq$ 8.4–8.6), it rises to much higher levels, as high as 0.4 dex for high oxygen abundances (O $\geq$ 8.8). It is due to the fact that high oxygen abundance PN have low temperatures, and thus intrinsically weak [OIII] 436.3 lines, which are thus highly affected by the noise. This effect is clearly enhanced in comparison with Disk PN, due to the high redenning of Bulge PN.

It can be seen as well that the uncertainties go down as a general tendency with increasing excitation class.

The 3 high uncertainty PN, as far as the oxygen abundance is concerned, are PN G 001.4 + 05.3 (H1 - 15), PN G 358.2 + 04.2 (M3 - 8), and PN G 359.1 - 02.3 (M3 - 16). These 3 Planetary Nebulae could not have the important diagnostic line [OIII] 436.3 nm measured.

PN G 001.4+05.3. This Planetary Nebula has as well the [NII] 575.5 nm auroral line at a very low level. For this Planetary Nebula, it is the only temperature diagnostic line that is present. Thus, the uncertainty on the electron temperature in this PN is very high, as can be seen in Table 2.

PN G 358.2+04.2. This Planetary Nebula has a high interstellar reddening, and, which is worse, it is badly determined (uncertainty of 0.3 dex) (see Table 2). This uncertainty thus transmits itself to the intrinsic individual line intensities.

PN G 359.1-02.3. This Planetary Nebula is of low electronic temperature and density. The uncertainties on the derived parameters lie therefore on a higher level.

3.2.2. Uncertainties on the nitrogen abundances

No systematical tendency with the abundance can be seen. As well, no systematical tendency with the excitation class can

Table 3. Abundances of the observed PN. The abundances are given on a logarithmic scale, where 12 is the abundance of hydrogen. All the abundances are followed by our evaluations of the uncertainties from Monte–Carlo simulations (1σ). Abundances judged of low quality, because of a lack of data, are followed by a semi-colon (:). As well, the excitation classes EC are mentioned.

PN G	EC	He	$\sigma_{\rm He}$	N	$\sigma_{\rm N}$	O	$\sigma_{\rm O}$	S	$\sigma_{\rm S}$	Ar	$\sigma_{\rm Ar}$	Cl	$\sigma_{\rm Cl}$
$000.1+04.3$	6	10.97	$\pm$0.02	8.09	$\pm$0.2	8.87	$\pm$0.1	6.69	$\pm$0.2	6.44	$\pm$0.1	-	-
$000.2-01.9$	3	10.98 :	$\pm$0.01	7.89	$\pm$0.1	8.61	$\pm$0.2	6.99	$\pm$0.2	6.32 :	$\pm$0.1	5.03	$\pm$0.3
$000.7+03.2$	7	11.09	$\pm$0.02	8.61	$\pm$0.1	9.00	$\pm$0.3	7.30	$\pm$0.3	6.85	$\pm$0.2	-	-
$001.2-03.0$	<2	9.89 :	-	8.52	$\pm$0.1	8.85	$\pm$0.3	6.92 :	$\pm$0.1	5.53 :	$\pm$0.3	-	-
$001.4+05.3$	4	11.00 :	$\pm$0.03	7.43	$\pm$0.3	8.69	$\pm$1.0	6.75	$\pm$0.9	6.27 :	$\pm$0.5	-	-
$002.6-03.4$	<2	10.01 :	-	8.56	$\pm$0.1	8.83	$\pm$0.4	6.86 :	$\pm$0.2	5.47 :	$\pm$0.3	-	-
$002.7-04.8$	6	11.18	$\pm$0.01	8.40	$\pm$0.1	8.65	$\pm$0.1	6.98	$\pm$0.1	6.55	$\pm$0.1	5.17	$\pm$0.2
$005.0+04.4$	5	11.13 :	$\pm$0.01	8.72	$\pm$0.2	8.90	$\pm$0.2	7.11	$\pm$0.1	6.70	$\pm$0.1	5.37	$\pm$0.2
$351.1+04.8$	4	11.03	$\pm$0.01	8.19	$\pm$0.2	8.73	$\pm$0.2	7.03	$\pm$0.2	6.42	$\pm$0.2	5.22	$\pm$0.3
$355.1-02.9$	6	11.00	$\pm$0.01	8.21	$\pm$0.1	8.77	$\pm$0.1	6.77	$\pm$0.1	5.86 :	$\pm$0.1	4.77 :	-
$355.2-02.5$	5	11.03 :	$\pm$0.01	8.21	$\pm$0.1	8.75	$\pm$0.1	6.77	$\pm$0.1	6.19	$\pm$0.1	5.02 :	-
$355.4-02.4$	6	11.13	$\pm$0.01	8.61	$\pm$0.2	8.90	$\pm$0.2	7.26	$\pm$0.1	6.76	$\pm$0.2	5.39	$\pm$0.3
$355.6-02.7$	5	10.98 :	$\pm$0.01	7.68	$\pm$0.1	8.55	$\pm$0.1	6.46	$\pm$0.1	6.11	$\pm$0.1	4.81	$\pm$0.2
$355.7-03.0$	5	11.09	$\pm$0.02	8.51	$\pm$0.1	8.82	$\pm$0.1	6.99	$\pm$0.1	6.53	$\pm$0.1	5.16	$\pm$0.2
$356.2-04.4$	6	11.04	$\pm$0.01	8.28	$\pm$0.2	8.80	$\pm$0.1	6.99	$\pm$0.1	6.30	$\pm$0.1	4.93	$\pm$0.2
$356.5-03.9$	2	10.60	-	7.82	$\pm$0.1	8.67	$\pm$0.2	6.90	$\pm$0.2	5.94 :	$\pm$0.1	4.95	$\pm$0.3
$356.5-02.3$	<2	9.88 :	-	8.22	$\pm$0.1	8.86	$\pm$0.2	6.74 :	$\pm$0.1	5.44 :	$\pm$0.3	-	-
$357.4-03.5$	6	11.00	$\pm$0.01	7.48	$\pm$0.1	8.54	$\pm$0.3	6.68	$\pm$0.2	6.12	$\pm$0.1	4.94	$\pm$0.4
$357.4-03.2$	6	11.09	$\pm$0.04	8.81	$\pm$0.2	8.91	$\pm$0.1	7.30	$\pm$0.1	6.64	$\pm$0.1	5.37	$\pm$0.3
$358.2+03.5$	5	10.95	$\pm$0.01	7.87	$\pm$0.2	8.62	$\pm$0.1	6.74	$\pm$0.2	5.78	$\pm$0.1	4.61 :	-
$358.2+03.6$	6	11.00	$\pm$0.01	8.17	$\pm$0.1	8.76	$\pm$0.1	6.74	$\pm$0.1	6.37	$\pm$0.1	4.97 :	-
$358.2+04.2$	4	11.08 :	$\pm$0.04	8.08	$\pm$0.2	8.55	$\pm$0.5	6.75	$\pm$0.5	6.36	$\pm$0.3	-	-
$358.3+03.0$	6	10.92	$\pm$0.03	8.08	$\pm$0.1	8.32	$\pm$0.1	6.62	$\pm$0.1	6.09	$\pm$0.1	-	-
$358.7-05.2$	6	11.01	$\pm$0.01	8.09	$\pm$0.1	8.80	$\pm$0.1	6.70	$\pm$0.1	6.38	$\pm$0.1	4.95 :	-
$358.9+03.2$	5	11.06	$\pm$0.01	8.47	$\pm$0.1	8.80	$\pm$0.1	7.09	$\pm$0.1	6.56 :	$\pm$0.1	5.18	$\pm$0.3
$358.9+03.4$	4	11.07 :	$\pm$0.01	8.24	$\pm$0.1	8.47	$\pm$0.1	6.86	$\pm$0.1	6.52 :	$\pm$0.1	-	-
$359.1-02.3$	4	10.97 :	$\pm$0.02	7.88	$\pm$0.3	8.90	$\pm$0.4	6.84	$\pm$0.4	6.27 :	$\pm$0.2	-	-
$359.3-03.1$	3	10.90 :	$\pm$0.03	7.94	$\pm$0.2	8.65	$\pm$0.5	7.09	$\pm$0.4	6.18 :	$\pm$0.2	5.09	$\pm$0.4
$359.7-02.6$	5	10.99 :	$\pm$0.02	7.90 :	$\pm$0.1	8.36 :	$\pm$0.2	6.63 :	$\pm$0.2	5.98 :	$\pm$0.1	-	-
$359.7-01.8$	6	10.93	$\pm$0.02	7.71	$\pm$0.1	8.45	$\pm$0.1	6.53	$\pm$0.2	5.62 :	$\pm$0.1	-	-

be seen. The envelope of the uncertainty level remains fairly constant at $\simeq 0.2$ dex.

3.2.3. Uncertainties on the helium abundances

Uncertainties on helium abundances show a clear tendency to decrease with increasing abundance. The emission mechanism for helium lines is mainly recombination. Although collisional excitation and reabsorbtion can have a secondary influence for the He I lines, the helium abundance is basically a function of the ratio of the helium lines to the hydrogen lines. The S/N ratio increasing with the intensities of helium lines (relative to Hβ), the uncertainty on the helium abundance should decrease with increasing abundance, which is exactly what is observed.

The mean uncertainties on the helium abundances from our sample are thus 0.03–0.02 dex, following the helium abundance.

Two PN have higher uncertainties on their helium abundances, of the order of 0.04 dex: PN G 357.4 - 03.2 (M2 - 18), and PN G 358.2 + 04.2 (M3 - 8).

The high uncertainty on the He abundance of PN G 358.2 + 04.2 is due to the high uncertainty of its reddening, as is the case for the uncertainty on its oxygen abundance.

On the other hand, the uncertainty on the helium abundance of PN G 357.4-03.2 is certainly over-evaluated: its high value is due to the fact that it is one of the only PN in the sample with measured He I 402.6 and 728.1 nm lines. Due to their faint intensities, these lines are measured in low S/N conditions. Therefore, they enhance the level of the uncertainty. We derived as well the He abundance for this PN without these two lines, and it did not change significantly.

3.2.4. Uncertainties on the sulphur, argon and chlorine abundances

The uncertainties on the sulphur and argon abundances generally follow, although not as clearly, the tendencies of the uncertainties on the oxygen abundances, with an envelope of the uncertainties of 0.2–0.3 dex. This is due to the chain of ICFs leading to the elemental abundances of sulphur and argon.

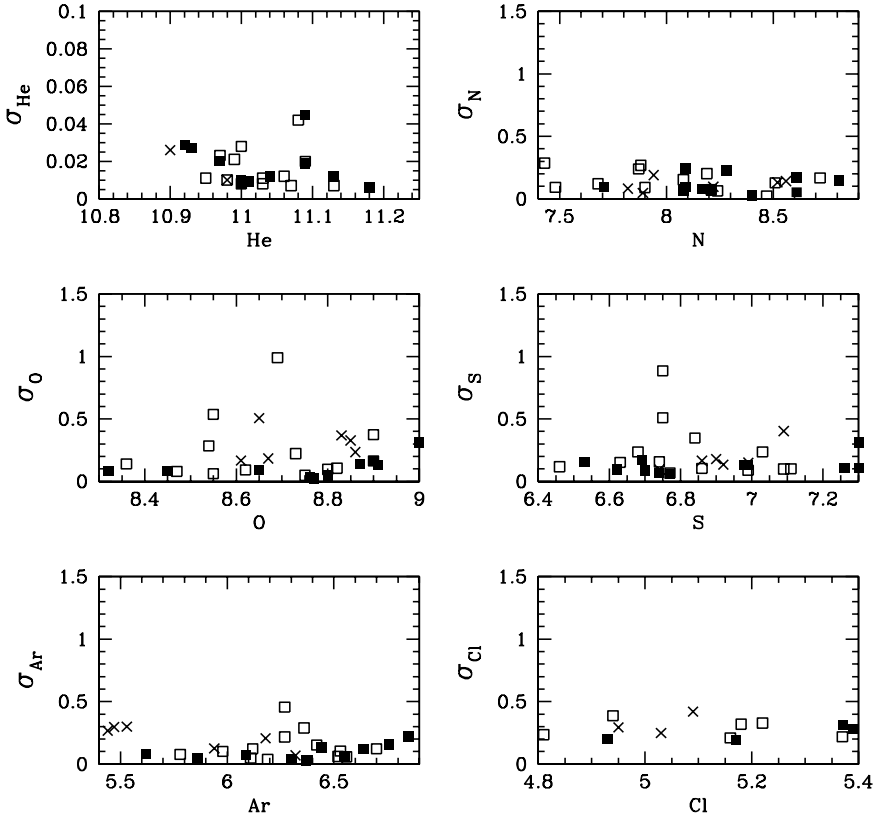

Fig. 1. Estimated uncertainties on the derived abundances for the individual PN. High excitation class PN (EC=6-7) are represented by filled squares, medium excitation class PN (EC=4-5) by open squares, and low excitation class PN (EC$\leq$ 3) by crosses.

As well, the few Planetary Nebulae that are well above these uncertainties are the same as in the case of oxygen, for the same reasons.

It should be added that the uncertainties on sulphur are clearly underevaluated, because of the inadequacy of the sulphur ICF, as quoted in Cuisinier et al. (1996). The uncertainty on the argon abundance should as well be underevaluated, to a lesser extent: The ICF on argon shows a systematic effect of $\simeq$ 0.1 dex (Köppen et al. 1991).

Finally, the chlorine abundances lie at higher uncertainty levels than the other ones, at 0.3–0.4 dex, with no systematic tendency, neither with abundance, nor with excitation class. This is due to the faintness of the chlorine lines – which are measured at much lower S/N ratios than the other ones.

Furthermore, the levels of the lines are so low that systematic effects should as well be present, over–evaluating their intensities, as quoted in Rola & Stasinska (1994).

3.3. Comparison with other data

There are five sources of Planetary Nebulae abundances determinations that present common data with our sample: Aller & Keyes (1987), Costa et al. (1996), Köppen et al. (1991), Ratag et al. (1997), and Webster (1988). The comparison with these four samples will be discussed below.

Köppen et al. (1991) spectra are of survey nature, and generally therefore of low quality. They will thus not be further discussed here.

Ratag et al. (1997) joined observations of them, made on various sites, with already existing abundances, in order to build a sample of Galactic Bulge Planetary Nebulae. However, their abundances compare very badly with ours. The comparison is made dificult by the lack of common objects with measured important diagnostic lines, like [OIII] 436.3nm.

However, the reasonable comparison with other good samples from the literature (Webster 1988, Aller & Keyes 1987, Costa et al. 1996) gave us some confidence in our parameters and abundance determinations.

We have 11 objects in common with Webster (1988), 2 with Aller & Keyes (1987) (PN G 002.7 - 04.8 = M 1 - 42 and PN G 356.2 - 04.4 = Cn 2 - 1) and 1 with Costa et al. (1996) (Cn 2 - 1). Fig. 2 shows the comparison of their data with ours for the helium abundance, Fig. 3 for the oxygen abundance and 4 for the nitrogen abundance.

3.3.1. Helium abundances

A slight systematic tendency exists for helium, our abundances being lower by $\simeq 0.01$ dex than theirs, especially Webster's ones – but this systematic tendency is well within our estimation of the uncertainty on the abundances of our data. The dispersion around this mean tendency is of 0.01 dex as well.

3.3.2. Oxygen abundances

Also for oxygen, there is a slight systematic tendency, our abundances being systematically lower. The mean difference is of

$\simeq 0.1$ dex, here as well, well within our estimation of the uncertainty on the oxygen abundances.

It should be added that this systematic tendency clearly increases with the oxygen abundance, being much stronger for oxygen rich PN. Although only 3-4 objects are concerned, the difference rises up to 0.2-0.3 dex for O/H> 9 (*literature* abundances).

If those objects are removed, the systematic tendency nearly disappears. This could indicate a systematic overevaluation of the oxygen abundance for oxygen rich PN from other studies. However, we cannot be conclusive about this point, because of the small number of objects involved, and because our evaluation of the random uncertainty for such objects is of the same order, or even higher.

For two of these object (PN G 000.7 + 03.2 = M 2 - 21 and PN G 358.2 + 04.2 = M 3 - 8), the usual diagnosis line [OIII] 436.3 could not be measured. Furthermore the [NII] 575.5 line, on which the electron temperature evaluation of these PN rely, was measured in such low S/N conditions that the error bars on the oxygen abundances are huge (respectivaly 0.3 and 0.5 dex!). Thus, the increase of the systematic tendency with oxygen abundance might not be so high.

Cn 2 - 1 (= PN G 356.2 - 04.4) on the other hand has been observed in relatively good conditions by Aller & Keyes (1987), with measurements of [OIII] 436.3 and [NII] 575.5 at a reasonable S/N ratio. These lines are also present in our observation of this Planetary Nebula, at a reasonable S/N and the oxygen abundance derivations are very different (0.8 dex!). We attribute the difference to the contamination of [OIII] 436.3nm line by Hg 435.9 from the city lights in Aller & Keyes observations. This contamination affects their deconvolution and measurement of the [OIII] 436.3 line, and hence their evaluation of the [OIII] electron temperature.

The observation of M 1 - 42 by Costa et al. (1996) also presents a higher oxygen abundance. We attribute this to their underestimation of the reddening, leading to an overevaluation of the intrinsic [NII] 658.4, 654.8 nm lines intensities. Thus, their [NII] electron temperature is underevaluated. Because they did not observe [OIII] 436.3 nm, they adopted the [NII] temperature for the [OIII] zone, leading to an overevaluation of the O^{++} abundance, and hence of the oxygen abundance. They also find a O^{++}/O^{+} ratio which very low, leading through the ICF to a correct nitrogen abundance.

Thus, taking away these objects, the dispersion of the oxygen abundance is of the order of 0.1–0.2 dex, well within our estimation of the random errors.

3.3.3. Nitrogen abundances

Looking at the data from the literature as a whole, our abundances compare within 0.2 dex with the abundances deduced by these authors, well within the generally quoted accuracy of PN abundances determination in the literature. No systematic tendency can be seen.

However, the two PN observed in common with Aller & Keyes 1987, Cn 2 - 1 (= PN G 356.2 - 04.4) and M 1 - 42 (= PN G 000.7 - 03.2), present systematically lower abundances (by $\simeq 0.4$ dex).

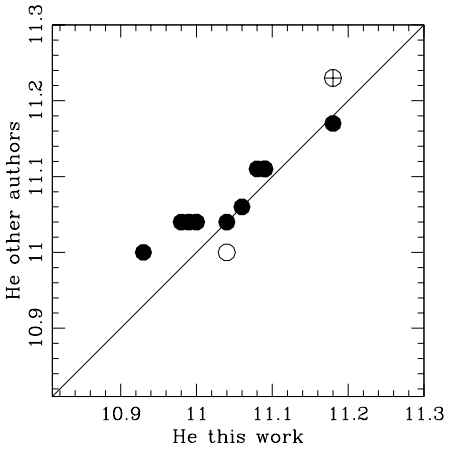

Fig. 2. Comparison of our determinations of the helium abundances with determinations from other authors. The helium abundances are represented on a logarithmic scale, where 12 is the hydrogen abundance. Filled circles stand for data from Webster (1988), open circles for data from Aller & Keyes 1987 and the cross for the common PN with Costa et al. (1996)

The nitrogen abundance is lower in Cn 2 - 1 because of the uncertain deconvolution of [OIII] 436.3 nm, leading to an incorrect O^{++} abundance, that reflects itself in the nitrogen abundance through the ICF.

The case of M 1 - 42 is a bit more tricky, because the nitrogen abundance is very different, whereas the oxygen abundance is very similar (in Aller & Keyes 1987). This can be explained by the fact that the [NII] 575.5 nm is *overestimated* by a factor of 10, leading to a very high [NII] temperature (in their observations). This combines with the problems in the deconvolution of [OIII] 436.3 nm. The measurement of this line is even qualified as uncertain by the authors, and therefore may well be underestimated, leading to an underestimation of the [OIII] temperature, and to an overestimation of the [OIII] zone abundances. The combination of these two effects gives a correct oxygen abundance, but overevaluates the nitrogen abundance.

4. Abundances distributions and discussion

4.1. Oxygen, sulphur and argon abundances

Oxygen, sulphur and argon are not synthetised in the progenitors of the Planetary Nebulae. Thus, these elements reflect the composition of the interstellar medium at the time when the progenitor star was born – and allow us to trace its chemical evolution.

In order to see wether the Bulge was chemically more or less evolved than the Disk, from the point of view of PN, we compared the abundances of these elements in our Bulge sample with the abundances of a Disk PN sample, taken from Maciel & Köppen (1994). We took this sample as a “best compromise”, because the Disk does clearly not constitue one unique population, but rather several ones. The variety of populations of the

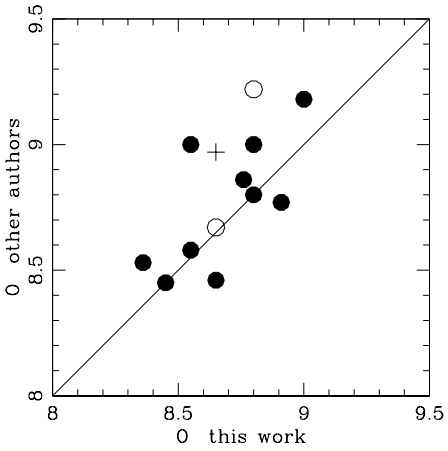

Fig. 3. Comparison of our determinations of the oxygen abundances with determinations from other authors. The symbols are the same than in Fig. 2

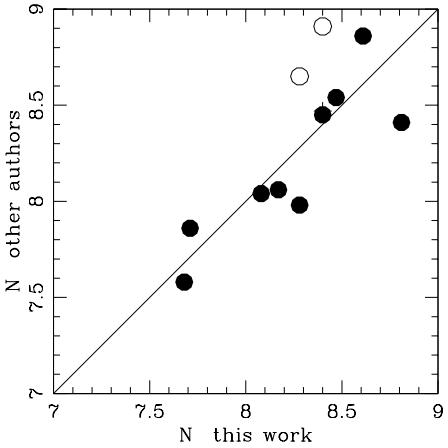

Fig. 4. Comparison of our determinations of the nitrogen abundances with determinations from other authors. The symbols are the same than in Fig. 2

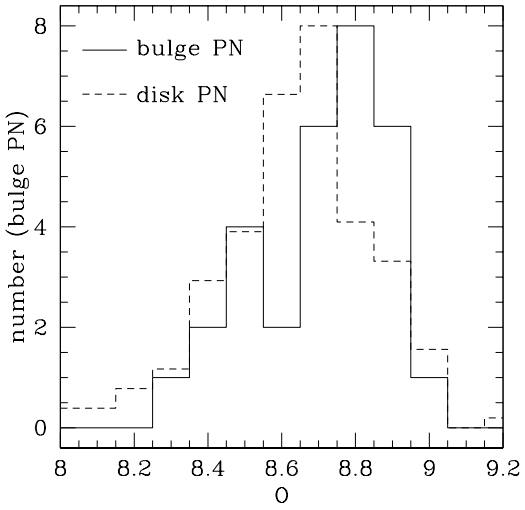

Fig. 5. Oxygen abundances for PN in the Bulge and in the Disk. The Bulge sample contains 30 PN, the Disk sample 198 PN. The vertical scale shows the number of objects in the Bulge sample.

Disk reflects itself in the radial abundances gradients (Maciel & Köppen 1994, Köppen et al. 1991, Faúndez-Abans & Maciel 1986). The effect of these gradients is to smooth and spread the abundance distributions over the Disk, but they do not change the form of the Disk abundance distributions as a whole. We resolved to adopt the abundances published in Maciel & Köppen 1994, because they represent the most comprehensive sample of PN abundances to this date. Through this choice, we hope to minimize systematic effects due to the choice of PN at a particular place in the Galaxy rather than at another one.

We found that the oxygen abundances in the Bulge PN are comparable to the abundances in oxygen in the Disk PN, the high abundance PN in the Bulge (O/H≃8.8–9.0) being slightly more numerous, as can be seen in Fig. 5. The mean abundance we encountered in the Bulge ($\langle \mathrm{O/H} \rangle = 8.71$) is also similar to the mean abundances that can be encountered in the youngest populations of the Disk, either in type I PN in the Disk (Costa et al. 1996), or in HII regions or B stars (Shaver et al. 1983, Smartt & Rolleston 1997, Maciel & Quireza 1999).

From the stellar point of view, it seems that the very high metallicities that were encountered in the Bulge from low resolution data in earlier studies (up to $[\mathrm{Fe/H}] \simeq +1\,\mathrm{dex}$)(Whitford & Rich 1983, Rich 1988, Geisler & Friel 1992) were really extrapolated too far. High resolution abundance studies have shown that the highest iron abundances that can be encountered, either in the Disk or in the Bulge giants, are of the order of $[\mathrm{Fe/H}] \simeq +0.6\,\mathrm{dex}$ (Mc William & Rich 1994, Castro et al. 1995, 1996, 1997). Mc William & Rich (1994) rescaled the low resolution study of Rich (1988), and encountered an iron abundance distribution that is similar to that of Mc William (1990) Disk giants sample, with a mean abundance of $\langle [\mathrm{Fe/H}] \rangle = -0.23\,\mathrm{dex}$. Within errors, this is similar to the mean iron abundance that can be encountered from G–dwarfs in the solar neighbourhood (Pagel 1989, 1997, Rocha-Pinto & Maciel 1996). A closer inspection of the data shows that if the mean abundances are similar, the high abundance stars ($[\mathrm{Fe/H}] \geq 0\,\mathrm{dex}$) are slightly more frequent in the Bulge than in the solar neighbourhood G-dwarfs. The solar neighbourhood G-dwarfs can be considered to be more representative of the Disk iron abundances than Mc William giants, because Mc William giants were selected on luminosity criteria, and are therefore biased in favour of massive stars, that should be slightly more metal-rich, as stated in Mc William & Rich (1994).

Recently, Sadler et al. (1996) made a new low resolution spectroscopical survey of a much larger sample than Rich (1988), and they encountered a slightly higher value of the mean iron abundance ($\langle [\mathrm{Fe/H}] \rangle = -0.11\,\mathrm{dex}$). However, they have a significant fraction of very high metallicity stars ($[\mathrm{Fe/H}] \geq 0.6\,\mathrm{dex}$), that pushes their mean iron abundance to high values. We thus prefer the Rich (1988) sample, rescaled to Mc William & Rich (1994) values, which we find to be in better agreement with the iron upper abundance limit from high resolution studies.

Thus, the oxygen abundances in PN behave like the iron abundances in stars, when the Bulge and the Disk populations are compared: the distributions are similar, high abundance objects being slightly over-numerous in the Bulge.

This is somehow unexpected from a theoretical point of view: the rapid star formation history of the Bulge, as would be expected for an old population, should enhance the nucleosynthesis products of supernovae of type II over thos of supernovae of type Ia, as the α elements (Matteucci & Brocatto 1990). Thus, oxygen should be enhanced over iron in the Bulge, contrarely to what seems to appear from the comparison of them stellar and the PN abundances in the Bulge and in the Disk. The same effect appears in the Mc William & Rich (1994) high resolution observations of Bulge giants. they found solar values for their [O/Fe] ratios. More generally, the α element pattern that they encountered in the Bulge is rather puzzling: some of their α elements are indeed enhanced, (like Mg and Ti), as would be expected from a rapid evolution, and others are not (O, Ca and Si). Idiart et al. (1996) also encountered an enhanced magnesium abundance in their integrated spectrum in Baade's window.

Aluminium is also enhanced in Mc William & Rich Bulge giants, thus the possibility of oxygen depleting processes should not be discarded. The results of such depleting processes have actually been observed in some globular cluster giants (Kraft et al. 1995). However, as stated in Richer et al. (1998), such processes are very unlikely to have occurred in the in the Bulge PN progenitors, because they would also have dramatically enhanced the nitrogen abundances, whereas as we will see in the next section, our Bulge PN have *low* N/O ratios, and never reach the values observed in oxygen depleted giants. ($[\mathrm{N/O}] \geq 1$, e.g. $\mathrm{N/O} \geq 0.1$, adopting Anders & Grevesse (1989) values for the solar abundances, according to Kraft et al. (1995) or Denissenkov et al. (1998)). Thus, we can consider that the oxygen abundances that we encountered in the Bulge PN have not been polluted by their progenitor nucleosynthesis, and really represent pristine material.

We also analysed the abundances in sulphur and argon. As in the Disk PN (Faúndez–Abans & Maciel, 1986, Cuisinier et al. 1996), we found them well correlated with the oxygen abundances. However, these abundances, suffer from higher uncertainties than the oxygen abundances due to the uncertainties on their ICFs. Within these uncertainies, they do not contradict the results from the oxygen abundances.

4.2. Helium and nitrogen abundances

Helium and nitrogen, contrarely to oxygen, sulphur, and argon, are synthetized in the progenitors of PN. Thus, these elements do not allow us to trace the chemical composition of the interstellar medium when the progenitor star was born, and hence they do not allow us to trace the chemical evolution of the interstellar medium.

On the other hand, and although it is not yet well quantified theoretically, the enrichment in these elements should be connected with the mass of the progenitors, and thus, with their ages (Cazetta & Maciel 1999, Stasinska & Tylenda 1990, Kaler 1983, 1985, Peimbert & Torres–Peimbert 1983, Aller 1987 et al.).

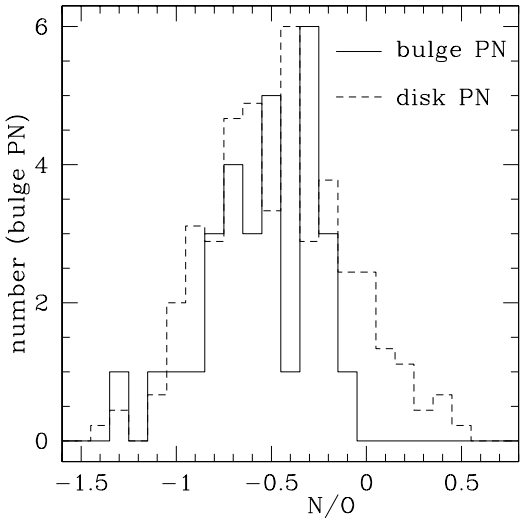

Fig. 6. N/O ratio for PN in the Bulge and in the Disk. The Bulge sample contains 30 PN, the Disk sample 198 PN.

The N/O ratio abundance ratio distribution should therefore reflect a mixture of the chemical evolution of nitrogen and oxygen before progenitor stars were formed, (2) the progenitor own nucleosynthesis.

It is noteworthy that the highest metallicity (e.g. oxygen abundance) galaxies do not produce N/O ratios higher than $\mathrm{N/O} \simeq -0.25$ (Vila–Costas & Edmunds 1993). Within errors, this is also the upper limit of the N/O distribution of our sample (Fig. 6).

However, the Disk PN N/O ratio distribution extends to much higher values – due to the nucleosynthesis of massive progenitor stars (The Kolmogorov–Smirnoff probability that the N/O distributions are different is 74%). (The oxygen abundances in the Disk were taken from Maciel & Köppen 1994, the nitrogen abundances from Maciel & Chiappini 1994, who list them for the PN from Maciel & Köppen (1994) sample.) Thus, the most recent population of PN in the Disk is clearly absent from the Bulge. This is what should be expected from stellar observations, showing that the turnoff lies around $\mathrm{V} - \mathrm{I} \simeq 0.6$ (Ortolani 1998), and is therefore an old population.

The helium abundances although not as clear, show a similar effect, as can be seen in Fig. 7: The most abundant objects that are present in in the Disk are absent in the Bulge. The distribution encountered in the Bulge compares with the Disk PN, if the high helium abundance type I PN are excluded.

We see that the mean value that we encounter, $\langle \mathrm{He/H} \rangle = 0.108$ (on a linear scale, considering only our best data), is lower than the pristine helium abundance predicted by chemical evolution models for the Bulge ($\mathrm{He/H} \simeq 0.12$)(Catelan & de Freitas Pacheco 1996). Helium abundances can only be obtained from indirect methods for stars in the Bulge, like differential counts in color magnitude diagrams. Although they can therefore considered to be not as trustworthy as the nebular abundances, good quality data seem

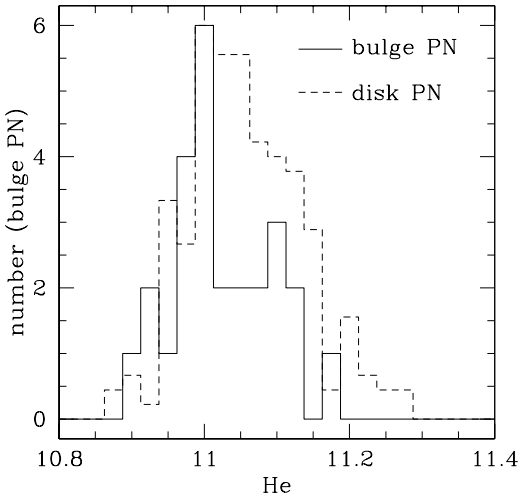

Fig. 7. He abundances for PN in the Bulge and in the Disk. The Disk sample contains 198 PN, the Bulge sample contains 17 PN (only PN with good helium abundances determinations, with EC$\geq$4 have been considered).

to favour low helium abundance values (He/H=0.098) (Minniti 1995), although higher values have been reported from lower quality data (Renzini 1994).

It seems that here as well, helium does not follow the overproduction predicted by chemical evolution models for a prompt enrichment.

5. Conclusions

We observed a sample of 30 Planetary Nebulae in the Galactic Bulge with high quality spectroscopy, for which we derived plasma parameters, and abundances of O, S, Ar,Cl, N, and He.

We evaluated random uncertainties with appropriate simulations, which were for these highly reddened Planetary Nebulae of the order of 0.02 dex for helium, of 0.2 dex for oxygen, sulphur, and argon, and of 0.4 dex for chlorine.

We compared the abundances we obtained with abundances derived by other authors, and our abundances fitted well within our estimations of the uncertainties.

We compared the abundances in O, S, Ar of the Planetary Nebulae from our Galactic Bulge sample with the abundances in Planetary Nebulae from the Galactic Disk. We found them to be comparable, Planetary Nebulae with high abundances in these elements being slightly more numerous – which is compatible with the findings from the stars.

The abundances in N/O and He showed a lack of high N/O and high He Planetary Nebulae in the Galactic Bulge, suggesting that the Bulge Planetary Nebulae have old progenitor stars, and here as well are similar to the stellar population.

Thus, the main results that appear from our observations are that: (1) The abundances in O, S, and Ar do not contradict the stellar observations in the Bulge (2) From the N/O ratio derivations, it seems that the Bulge Planetary Nebulae are an old population, like the stars.

If the abundances that can be derived from stars and Planetary Nebulae in the Galactic Bulge are not contradictory, the pattern that is found can still be considered as very puzzling: if there is no doubt that the most recent population that is encountered in the Galactic Disk does not appear either in the Planetary Nebulae or in the stars, some elements favour a prompt chemical enrichment (Mg and Ti), and other favour a much slower chemical evolution history (He, O, Si, S, Ar and Ca).

Acknowledgements. F.C. thanks FAPESP for financial support, through the grant 95/04766–8, and the Instituto Astronômico e Geofisico da USP, for hospitality during his stay as a post–doctoral fellow. W.J.M. thanks FAPESP and CNPq for partial financial support. We would like to thank as well the referee, J.A. de Freitas Pacheco, for helpful suggestions, and G. Stasinska, for fruitful discussions.

References

Acker A., Köppen J., Stenholm B., Raytchev B., 1991, A&AS 89, 237
Aller L., Keyes C., Maran S., 1987, ApJ 320, 159
Aller L., Keyes C., 1987, ApJS 65, 405
Anders E., Grevesse N., 1989, Geochimica & Cosmochimica Acta 53, 197
Baldwin J.A., Stone R.P.S., 1984, MNRAS 206, 241
Castro S., Barbuy B., Bica E., et al., 1995, A&AS 111, 17
Castro S., Rich R.M., Mc William A., et al., 1996, AJ 116, 2439
Castro S., Rich R.M., Grenon M., et al., 1997, AJ 114, 376
Catelan M., de Freitas Pacheco J.A., de França Jr. J.A., 1996, A&A 313, 924
Cazetta J.O., Maciel W.J., 1999, in preparation
Colina L., Bohlin R., 1994, AJ 108, 1931
Costa R., de Freitas Pacheco J.A., de França Jr. J.A., 1996, A&A 313, 924
Cuisinier F., Acker A., Köppen, 1992, In: The Feeedback of chemical evolution on the stellar content of Galaxies. p. 99
Cuisinier F., Acker A., Köppen J, 1996, A&A 307, 215
Denissenkov P.A., Da Costa G.S., Norris G.E., Weiss A., 1998, A&A 333, 928
Faúndez-Abans M., Maciel W., 1986, 158, 228
Geisler D., Fried E.D., 1992, AJ 104, 128
Hamuy M., Walker A., Suntzeff N., et al., 1992, PASP 104, 533
Hamuy M., Suntzeff N., Heathcote S., et al., 1994, PASP 106, 566
Idiart T., de Freitas Pacheco J.A., Costa R.D.D., 1996, AJ 111, 1169
Kaler J., 1983, ApJ 271, 188
Kaler J., 1985, ARA&A 23, 89
Köppen J., Acker A., Stenholm B., 1991, A&A 248, 197
Kraft R.P., Sneden C., Langer G.E., et al., 1995, AJ 109, 2586
Maciel W., Köppen J., 1994, A&A 282, 436
Maciel W., Chiappini C., 1994, Ap&SS 219, 231
Maciel W., Quireza C., 1999, A&A 345, 629
Massey P., Strobel K., Barnes J., Anderson E., 1988, ApJ 328, 31
Matteucci F., Brocatto E., 1990, ApJ 365, 539
Mc William A., 1990, ApJS 74, 1075
Mc William A., Rich R.M., 1994, ApJS 91, 749
Minniti D., 1995, A&A 300, 109
Oke J., 1990, AJ 99, 1621
Ortolani S., 1998, In: Spite, Spite (eds.) Connecting the Distant Universe with the Local Fossil Record
Pagel B.E.J., 1989, In: Beckman, Pagel (eds.) Evolutionary phenomena in galaxies. Cambridge University Press, p. 201

Pagel B.E.J., 1997, In: Nucleosynthesis and Chemical Evolution of Galaxies. Cambridge University Press
Peimbert M., Torres-Peimbert S., 1983, IAU symp. 103, p. 233
Ratag M., Pottasch S., Dennefeld M., Menzies J., 1992, A&A 255, 255
Ratag M., Pottasch S., Dennefeld M., Menzies J., 1997, A&AS 126, 297
Renzini A., 1994, A&A 285, L5
Rich R.M., 1988, AJ 95, 828
Richer M.G., Mc Call M.L., Stasinska G., 1998, A&A 340, 67
Rola C., Stasinska G., 1994, A&A 282, 199
Rocha–Pinto, H., Maciel W., 1996, MNRAS 279, 447
Sadler E.M., Rich R.M., Terndrup D.M., 1996, AJ 112, 171
Shaver P.A., Mc Gee R.X., Newton L.M., et al., 1983, MNRAS 204, 53
Smartt S.J., Rolleston W.R.J., 1997, ApJ 481, L47
Stasinska G., Tylenda R., 1990, A&A 240, 467
Stone R.P.S., Baldwin J.A., 1983, MNRAS 204, 347
Stone R.P.S., 1977, ApJ 218, 767
Stone R.P.S., 1996, ApJS 107, 423
Vila–Costas M.B., Edmunds M.G., 1993, MNRAS 265, 199
Webster L., 1988, MNRAS 230, 377
Whitford A.E., Rich R.M., 1983, ApJ 274, 723